Dalton
www.rsc.org/dalton

The dimerisation of carbon disulfide on Fe centres. Some new tetrathiolene complexes of iron

Natalie L. Cromhout,[a] Anthony R. Manning,*[a] C. John McAdam,[b] Anthony J. Palmer,[a] Anne L. Rieger,[c] Philip H. Rieger,[c] Brian H. Robinson[b] and Jim Simpson[b]

[a] *Department of Chemistry, University College Dublin, Belfield, Dublin 4, Ireland. E-mail: Anthony.Manning@ucd.ie*

[b] *Department of Chemistry, University of Otago, PO Box 56, Dunedin, New Zealand. E-mail: Brobinson@alkali.otago.ac.nz; Jsimpson@alkali.otago.ac.nz*

[c] *Department of Chemistry, Brown University, Providence, RI 02912, USA*

Received 20th March 2003, Accepted 1st April 2003
First published as an Advance Article on the web 23rd April 2003

The thermolysis of $[Fe(L)_2(CO)_2(\eta^2\text{-}CS_2)]$ complexes (**1**) in refluxing benzene gives the blue tetrathiolene derivatives $[Fe_2(L)_4(CO)_2(C_2S_4)]$ (**2**) when L = $P(OPh)_3$, $P(OEt)_3$, $P(OPr^i)_3$, $PPh(OEt)_2$, $PPh_2(OEt)$. **2** are formed only when the phosphorus(III) ligands L readily dissociate from **1** and have cone angles between 109° and 133°. The two most stable are **2a** {L = $P(OPh)_3$, cone angle 128°} and **2c** {L = $P(OPr^i)_3$, cone angle 130°}. **2** have been characterised by IR, electronic and NMR spectroscopy and elemental analyses. Their UV-Vis spectra are dominated by an intense absorption band (ε = 13000–18000 $dm^3\ mol^{-1}\ cm^{-1}$) with λ_{max} = 640–690 nm. The labile triphenylphosphite ligands in **2a** can be replaced in part by CO. Spectroscopic data confirms that the unstable product, **3a**, contains a ligand set similar to that of **2a**. Electrochemical studies show that **2a** undergoes a one-electron reversible reduction to $[\mathbf{2a}]^{\bullet -}$ and a one-electron, irreversible oxidation. The UV-Vis spectrum of $[\mathbf{2a}]^{\bullet -}$ shows a very low energy absorption band at 2556 nm (3912 cm^{-1}) with ε = *ca.* 3600 $dm^3\ mol^{-1}\ cm^{-1}$ which is attributed to a charge transfer transition from the SOMO to an orbital with $\mu\text{-}C_2S_4$ character. The ESR spectrum of $[\mathbf{2a}]^{\bullet -}$ is consistent with the SOMO being an orbital of primarily $d_{x^2-y^2}$ character which is localised on one Fe atom. Under CO, one-electron reversible transfers are observed in the electrochemistry due to the redox series $[\mathbf{3a}]^{-/0/+}$. **2a** is oxidised by halogens to $[L_2(OC)(X)Fe(S_2C_2S_2)Fe(X)(CO)L_2]$ derivatives.

Introduction

The reaction of $[Fe_2(CO)_9]$ and $P(OPh)_3$ in refluxing carbon disulfide gave a dark green mixture from which could be isolated orange $[Fe\{P(OPh)_3\}_2(CO)_2(\eta^2\text{-}CS_2)]$.[1] The co-product giving rise to the green colour has now been isolated and found to be the deep blue tetrathiolene† complex $[\{(PhO)_3P\}_2(OC)Fe(S_2C_2S_2)Fe(CO)\{P(OPh)_3\}_2]$ (**2a**). The present paper describes the preparation, isolation, characterisation and structure of a series of these complexes.

There have been a number of reports of transition metal-promoted head-to-head dimerisation of CS_2. In $[\{Fe_2(CO)_6\}_2(C_2S_4)]$ the C_2S_4 moiety acts as two 1,1-dithiolate ligands to each of the two $Fe_2(CO)_6$ fragments with a C=C bond,[2] but more commonly C_2S_4 acts as a 1,2-dithiolene to two metal atoms in $M(S_2C_2S_2)M$ complexes where M = $Ni(\eta^5\text{-}C_5Me_5)$,[3] $Ti(\eta\text{-}C_5H_5)_2$,[4] and $Rh\{\eta^3\text{-}(Ph_2PCH_2)_3CMe\}^+$.[5] $(\eta^5\text{-}C_5Me_5)Rh(S_2C_2S_2)Rh(\eta^5\text{-}C_5Me_5)$ has been reported, but was prepared from $[Rh_2(\eta^5\text{-}C_5Me_5)_2Cl_4]$ and tetrathiooxalate salts.[6]

In related reactions, the reduction of $[Fe(L)_2(CO)_2\{\eta^2\text{-}C(S)SR\}]^+$ salts results in the dimerisation of their $C(S)SR^+$ ligands to $(RS)_2C_2S_2$. The product is $[Fe_2(L)_2(CO)_4\{\eta,\eta'\text{-}S_2C_2(SR)_2\}]$ or $[Fe(L)_n(CO)_{3-n}\{S_2C_2(SR)_2\}]$ (n = 1 or 2) depending on L and the reducing agent.[7] In the former the $(RS)_2C_2S_2$ ligands act as a 1,2-dithiolate $R'C(S^-)C(S^-)R'$ with a C=C, whereas in the latter it is a $R'_2C_2S_2$ dithiolene where R′ = SR. Similar compounds were first prepared from the reactions of dithietenes and iron carbonyls.[8]

Experimental

General procedures

Published methods or extensions thereof were used to prepare $[Fe_2(CO)_9]$,[9] and $[Fe(L)_2(CO)_2(\eta^2\text{-}CS_2)]$ where L is a P(III) ligand.[1,10] Other chemicals were purchased and used as received. Reactions were carried out in dried and deoxygenated solvents under an atmosphere of nitrogen at room temperature unless stated otherwise. They were monitored by IR spectroscopy using a Perkin-Elmer Paragon 2000 FTIR spectrometer. ^{1}H NMR spectra were obtained at 25 °C on a Jeol JNM-GX 270 spectrometer; ^{13}C NMR spectra at 30 °C on a Varian INOVA 500 MHz spectrometer operating at 126 MHz; and ^{31}P NMR spectra at 30 °C on a Varian INOVA 300 MHz spectrometer operating at 121 MHz. UV/Vis spectra were recorded on a Unicam UV2 spectrometer. Elemental analyses were carried out in the Microanalytical Laboratory of University College Dublin. Cyclic and square wave voltammetry in CH_2Cl_2 were performed for all compounds using a three-electrode cell with a polished disk, Pt (2.27 mm^2) as the working electrode; solutions were ≈10^{-3} M in electroactive material and 0.10 M in supporting electrolyte (triply recrystallised $Bu_4N^+PF_6^-$). Data was recorded on an EG & G PAR 273A or an AD Instruments Powerlab 4SP computer-controlled potentiostat. Scan rates of 0.05–1 V s^{-1} were typically employed for cyclic voltammetry and for Osteryoung square-wave voltammetry, square-wave step heights of 1–5 mV, a square amplitude of 15–25 mV with a frequency of 30–240 Hz. All potentials are referenced to decamethylferrocene; $E_{1/2}$ for sublimed ferrocene was 0.55 V. OTTLE spectra were obtained using Pt gauze electrodes in the thin layer cell of our own design.[11] To record ESR spectra (Bruker EMX X-band spectrometer) the compound was dissolved in a 1 : 1 mixture of $CH_2Cl_2/C_2H_4Cl_2$ with 0.1 M $Bu_4N^+PF_6^-$. The solution was reduced electrochemically in an *in situ* electrolysis cell in the cavity of the EPR spectrometer at room temperature.

Preparation of $[Fe_2\{P(OPh)_3\}_4(CO)_2(C_2S_4)]$ (2)

A mixture of $[Fe_2(CO)_9]$ (3.0 g; 8.24 mmol), $P(OPh)_3$ (10.2 g; 33 mmol), carbon disulfide (5 ml) and benzene (50 ml) was refluxed for 1.5 h. The volatiles were removed at reduced

† Tetrathiolene is used to differentiate the $MS_2C_2S_2M$ complexes from the dithiolene complexes $R_2C_2S_2M$.

DOI: 10.1039/b303186a

pressure and 100 °C to leave an oil that was extracted with diethyl ether (2 × 20 ml). The residue was recrystallised from chloroform–diethyl ether mixtures to give purple crystals of **2a**.Yield 1.5 g; 25%.

If [Fe{P(OPh)$_3$}$_2$(CO)$_2$(η^2-CS$_2$)] in benzene is refluxed for *ca*. 15 min **2a** may be isolated as above in a yield of 45–50%.

Other **2** may be prepared similarly by either method when P(OPh)$_3$ is replaced by L = (**b**) P(OEt)$_3$, (**c**) P(OPr^i)$_3$, (**d**) PPh(OEt)$_2$ and (**e**) PPh$_2$(OEt). Purification was generally carried out as above, but in some cases chromatography on alumina was used.

These reactions fail with other L = PMe$_3$, PBu$^n_3$, P(OMe)$_3$, and P(OCH$_2$)$_3$CMe which form [Fe(L)(CO)$_4$] or [Fe(L)$_2$(CO)$_2$-(η^2-CS$_2$)], whilst PPh$_3$, P(C$_6$H$_4$Me-4)$_3$, P(C$_6$H$_4$OMe-4)$_3$ and P(OC$_6$H$_4$Cl-4)$_3$ give highly coloured products which are not **2**.They could not be identified and were not investigated further.

[Fe$_2${P(OPh)$_3$}$_4$(CO)$_2$(C$_2$S$_4$)]·½CHCl$_3$, 2a·½CHCl$_3$. Yield 25% (Found: C 57.1, H 3.8, Fe 7.1, P 7.8, S 8.5; C$_{76.5}$H$_{60.5}$Fe$_2$-O$_{14}$P$_4$S$_4$Cl$_{1.5}$ requires: C 56.6, H 3.7, Fe 6.9, P 7.6, S 7.9%). IR ν/cm^{-1}: ν(CO) 1962 (CH$_2$Cl$_2$). ^{1}H NMR (CDCl$_3$): δ 7.0 [m, C$_6H_5$]. ^{13}C NMR (CDCl$_3$): δ 212.3 [t, J_{PC} = 31.1 Hz, *C*O], 193.8 [br s, *C*=*C*], 151.9, 129.6, 125.0, 121.9 [s, all O*C*$_6$H$_5$], ^{31}P NMR (CDCl$_3$): δ 162.5. UV/VIS (CH$_2$Cl$_2$): λ_{max}/nm (ε/dm^3 mol^{-1} cm^{-1}) 517 (4,600), 677 (17,300).

[Fe$_2${P(OEt)$_3$}$_4$(CO)$_2$(C$_2$S$_4$)], 2b. Yield 11% (Found: C 34.4, H, 6.0, P 13.1; C$_{28}$H$_{60}$Fe$_2$O$_{14}$P$_4$S$_4$ requires: C 34.1, H 6.1, P 12.6%). IR ν/cm^{-1}: ν(CO) 1942. ^{1}H NMR (CDCl$_3$): δ 3.77 [2, m, CH_2], 1.13 [3, t, J_{HH} = 6.9 Hz, CH_3]. ^{31}P NMR (CDCl$_3$): δ 175.4. UV/VIS (CH$_2$Cl$_2$): λ_{max}/nm (ε/dm^3 mol^{-1} cm^{-1}) 513 (4,600), 640 (17,300).

[Fe$_2${P(OPr^i)$_3$}$_4$(CO)$_2$(C$_2$S$_4$)], 2c. Yield 43% (Found: C 41.6, H, 7.4, P 11.1, S 11.1; C$_{40}$H$_{84}$Fe$_2$O$_{14}$P$_4$S$_4$ requires: C 41.7, H 7.3, P 10.8, S 11.1%). IR ν/cm^{-1}: ν(CO) 1935 (CH$_2$Cl$_2$). ^{1}H NMR (CDCl$_3$): δ 4.20 [1, m, C*H*], 1.12 [6, dd, J = 6.1 and 18.5 Hz, CH_3]. ^{13}C NMR (CDCl$_3$): δ 214.2 [t, J_{PC} = 36.0, *C*O], 183.5 [br s, *C*=*C*], 69.6 [s, *C*H$_3$], 24.3 [s, O*C*H]. ^{31}P NMR (CDCl$_3$): δ 171.9. UV/VIS (CH$_2$Cl$_2$): λ_{max}/nm (ε/dm^3 mol^{-1} cm^{-1}), 527 (8,500), 642 (15,800).

[Fe$_2${PPh(OEt)$_2$}$_4$(CO)$_2$(C$_2$S$_4$)]·CHCl$_3$, 2d·CHCl$_3$. Yield 19% (Found: C 42.9, H, 5.2, P 10.3, S 10.8; C$_{745}$H$_{61}$Fe$_2$O$_{10}$P$_4$S$_4$Cl$_3$ requires: C 43.8, H 5.0, P 10.1, S 10.4%). IR ν/cm^{-1}: ν(CO) 1938 (CH$_2$Cl$_2$). ^{1}H NMR (C$_6$D$_6$): δ 7.0 [5, m, C$_6H_5$], 3.4 [4, br, m, CH_2], 0.85 [6, br, m, CH_3]. ^{31}P NMR (CDCl$_3$): δ 195.6. UV/VIS (CH$_2$Cl$_2$): λ_{max}/nm (ε/dm^3 mol^{-1} cm^{-1}), 671 (13,200).

[Fe$_2${PPh$_2$(OEt)}$_4$(CO)$_2$(C$_2$S$_4$)], 2e. Yield 19% (Found: C 58.1, H, 4.8, P 9.1, S 10.9; C$_{40}$H$_{84}$Fe$_2$O$_{14}$P$_4$S$_4$ requires: C 58.0, H 4.8, P 10.0, S 10.3%). IR ν/cm^{-1}: ν(CO) 1930 (CH$_2$Cl$_2$). ^{1}H NMR (C$_6$D$_6$): δ 6.14–7.55 [10, m, C$_6H_5$], 3.41 [2, m, CH_2], 0.85 [3, t, J_{HH} = 6.6, CH_3]. UV/VIS (CH$_2$Cl$_2$): λ_{max}/nm (ε/dm^3 mol^{-1} cm^{-1}), 686 (13,600).

The reaction of [Fe$_2${P(OPh)$_3$}$_4$(CO)$_2$(C$_2$S$_4$)], 2a, with CO

CO gas was passed though a solution of **2a** (0.2 g; 0.13 mmol) in dichloromethane (20 ml) for *ca*. 5 min. IR spectroscopy showed that a new compound **3a** was formed but attempts to isolate it by removal of the solvent at reduced pressure led to the quantitative isolation of **2a**. [Ph$_3$C]BF$_4$ (0.045 g; 0.16 mmol.) was added to the reaction mixture which was filtered immediately, and the solvent removed at reduced pressure. The residue was extracted with benzene (2 × 10 ml). The mixture was filtered, and the solvent removed from the filtrate at reduced pressure to give purple crystals of the product, **3a**. It could not be purified as it decomposed rapidly both in the solid state and solution. However, **3a** is stable in solution in the presence of CO before the addition of [Ph$_3$C]BF$_4$ (above) and it is for this solution or a similar one in CDCl$_3$ that the following spectroscopic data were obtained: IR ν/cm^{-1} (relative peak heights): ν(CO), 2017 (10), 1976 (4, br) (CH$_2$Cl$_2$). ^{1}H NMR (CD$_2$Cl$_2$): δ 7.11 (br, m, C$_6H_5$). ^{13}C NMR (CD$_2$Cl$_2$): δ 210.2 [d, J(PC) = 24.1 Hz, *C*O], 209.3 [s, *C*O], 196.4 [s, *C*=*C*], 151.1, 130.0, 125.6, 125.2, 121.6, 121.1 [s, all O*C*$_6$H$_5$]. ^{31}P NMR (CDCl$_3$): δ 164.2 (s), 162.4 (s). UV-VIS (CH$_2$Cl$_2$): λ_{max}/nm (ε/dm^3 mol^{-1} cm^{-1}) 505 (5,100), 667 (20,600).

Reaction of [Fe$_2${P(OPh)$_3$}$_4$(CO)$_2$(C$_2$S$_4$)], 2a, with halogens

Iodine vapour from a solution of I$_2$ (0.050 g) in chloroform (3 ml) was allowed to diffuse into a filtered solution of **2a** (0.093 g, 0.06 mmol) in chloroform (4 ml) over a period of 96 h. A dark green solid was filtered off, washed with diethyl ether and dried. It analysed as [Fe$_2${P(OPh)$_3$}$_4$(CO)$_2$(C$_2$S$_4$)I$_2$], **4a(I)**, (yield 0.082 g, 75%). The reaction may be carried out with the same result by layering a chloroform solution (5 ml) of **2a** (0.093 g, 0.06 mmol) with one of I$_2$ (0.015 g, 0.06 mmol) in toluene (5 ml) and allowing it to stand at −18 °C in the dark for 96 h. If the iodine solution in chloroform, dichloromethane or toluene is added in a single aliquot to that of **2a** in the same solvent, a green solution from which **4a(I)** is obtained.

Comparable reactions of **2a** with PhICl$_2$ or [C$_5$NH$_6$]Br$_3$ (mole ratio 1 : 1) in dichloromethane gave [Fe$_2${P(OPh)$_3$}$_4$(CO)$_2$-(C$_2$S$_4$)Cl$_2$], **4a(Cl)**, or [Fe$_2${P(OPh)$_3$}$_4$(CO)$_2$(C$_2$S$_4$)Br$_2$], **4a(Br)**, in 75% and 65% yields respectively. The second of these was particularly unstable.

[Fe$_2${P(OPh)$_3$}$_4$(CO)$_2$(C$_2$S$_4$)I$_2$], 4a(I). Yield 75% (Found: C 49.8, H 3.4, P 6.9, S 7.5, I 13.5; C$_{76}$H$_{60}$Fe$_2$I$_2$O$_{14}$P$_4$S$_4$ requires: C 50.3, H 3.4, P 6.8, S 7.1, I 14.0%). IR (CH$_2$Cl$_2$): ν(CO) 2006 cm^{-1}. IR (KBr): ν(CO) 1997 cm^{-1}. UV/VIS (CH$_2$Cl$_2$): λ_{max}/nm (ε/dm^3 mol^{-1} cm^{-1}) 476 (6,100), 746 (11,000).

[Fe$_2${P(OPh)$_3$}$_4$(CO)$_2$(C$_2$S$_4$)Br$_2$], 4a(Br). Yield 65% (Found: C 50.8, H 3.3, P 7.4, S 7.6.5, Br 9.5; C$_{76}$H$_{60}$Fe$_2$Br$_2$O$_{14}$P$_4$S$_4$ requires: C 53.0, H 3.5, P 7.2, S 7.5, Br 9.3%). IR (CH$_2$Cl$_2$): ν(CO) 2005 cm^{-1}. IR (KBr): ν(CO) 2008 cm^{-1}.

[Fe$_2${P(OPh)$_3$}$_4$(CO)$_2$(C$_2$S$_4$)Cl$_2$], 4a(Cl). Yield 75% (Found: C 54.6, H 3.4, P 7.8, S 8.5, Cl 4.4; C$_{76}$H$_{60}$Fe$_2$Cl$_2$O$_{14}$P$_4$S$_4$ requires: C 55.9, H 3.7, P 7.6, S 7.9, Cl 4.3%). IR (CH$_2$Cl$_2$): ν(CO) 2006 cm^{-1}. IR (KBr): ν(CO) 2012 cm^{-1}. UV/VIS (CH$_2$Cl$_2$): λ_{max}/nm (ε/dm^3 mol^{-1} cm^{-1}) 440 (6,600), 708 (9,100).

Crystal structure determinations of [Fe$_2${P(OPh)$_3$}$_4$(CO)$_2$(C$_2$S$_4$)] (2a) and [Fe$_2${P(OPr^i)$_3$}$_4$(CO)$_2$(C$_2$S$_4$)] (2c)

Single crystals of **2a** and **2c** were grown from benzene/methanol and dichloromethane/methanol, respectively, and subject to an X-ray diffraction study. Data were collected on a Bruker SMART CCD diffractometer, processed using SAINT[12] with empirical absorption corrections applied using SADABS.[13] The structures were solved using SHELXS[14] and refined by full matrix least squares using SHELXL-97[14] and TITAN2000.[15] In both compounds the molecules lie on a centre of symmetry located at the midpoint of the C(1)–C(1a) bond of the C$_2$S$_4$ moiety so that refinement involved only half of the molecular unit. In the case of **2a**, after all of the non-hydrogen atoms were located, a difference map revealed several high peaks. This was consistent with positional disorder of the C(41)–C(46) phenyl ring, which was resolved by refining two unique positions for atoms C(42), C(43), C(45) and C(46) with occupancy factors f and f' which refined such that $f' = 1 - f$. The final value of f refined to 0.476(5). The crystal data and structure refinement details are given in Table 1.

CCDC reference numbers 194364 and 194365.

See http://www.rsc.org/suppdata/dt/b3/b303186a/ for crystallographic data in CIF or other electronic format.

Table 1 Crystal data and structure refinement for $[Fe_2\{P(OPh)_3\}_4(CO)_2(C_2S_4)]$, **2a**, and $[Fe_2\{P(OPr^i)_3\}_4(CO)_2(C_2S_4)]$, **2c**

Compound	**2a**	**2c**
Chemical formula	$C_{76}H_{60}Fe_2O_{14}P_4S_4$	$C_{40}H_{84}Fe_2O_{14}P_4S_4$
Formula weight	1561.06	1152.89
T/K	163(2)	146(2)
λ/Å	0.71073	0.71073
Crystal system	Triclinic	Triclinic
Space group	$P\bar{1}$	$P\bar{1}$
a/Å	10.609(6)	11.168(4)
b/Å	11.223(6)	11.255(4)
c/Å	16.205(9)	12.083(4)
α/°	91.665(7)	78.93(2)
β/°	92.351(8)	82.73(2)
γ/°	113.701(7)	86.46(2)
V/Å^3	1763.1(17)	1477.4(9)
Z	1	1
D_c/Mg m^{-3}	1.470	1.296
μ/mm^{-1}	0.687	0.793
Reflections collected	22761	7182
Independent reflections [R(int)]	7083 [0.0617]	5344 [0.1166]
Final R indices {$I>2\sigma(I)$]	$R_1 = 0.0496$, $wR_2 = 0.1105$	$R_1 = 0.0781$, $wR_2 = 0.1863$
R indices (all data)	$R_1 = 0.1047$, $wR_2 = 0.1227$	$R_1 = 0.0971$, $wR_2 = 0.1992$
Largest diff. peak and hole/e Å^{-3}	0.950 and −1.098	1.025 and −1.144

Results and discussion

The reactions carried out in the course of this work are summarised in Scheme 1. The $[Fe_2(L)_4(CO)_2(C_2S_4)]$ complexes, **2**, are blue or purple solids. They are soluble in organic solvents, but insoluble in water. None is particularly stable, but those where L = (**a**) $P(OPh)_3$, (**b**) $P(OEt)_3$, (**c**) $P(OPr^i)_3$, (**d**) $PPh(OEt)_2$, and (**e**) $PPh_2(OEt)$ could be characterised by elemental analyses, spectroscopy and, for **2a** and **2c**, X-ray crystallography. Other L {*e.g.* $P(OCH_2Ph)_3$} form **2**, but they are much less stable and could only be identified spectroscopically.

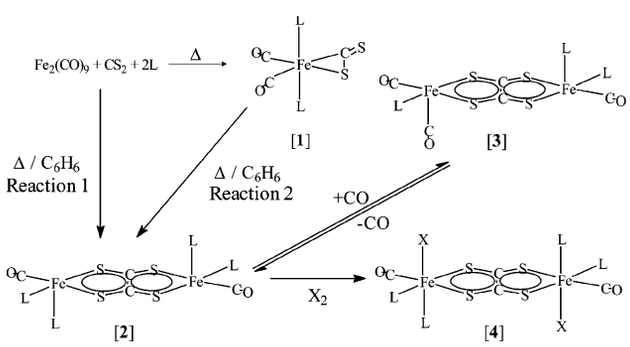

Scheme 1 Formation of $[Fe(L)_4(CO)_2(C_2S_4)]$, **2**, and their reaction with halogens.

Formation of $[Fe_2(L)_4(CO)_2(C_2S_4)]$ from CS_2

Phosphorus(III) ligands, L, react with $[Fe_2(CO)_9]$ in refluxing carbon disulfide solution to give $[Fe(L)_2(CO)_2(\eta^2\text{-}CS_2)]$ complexes, **1**, in good yield.[1,10] However, if benzene is added to the reaction mixture and the reflux continued for 1.5–3 h, the colour darkens (Reaction 1 in Scheme 1). $[Fe_2(L)_4(CO)_2(C_2S_4)]$ (**2**) complexes can be isolated as crystalline solids from the reaction mixtures in moderate to poor yields together with some $[Fe(L)(CO)_4]$, $[Fe(L)_2(CO)_3]$ and traces of unidentified coloured species.

It is implied by the above reactions that **2** are formed from **1**. This has been confirmed. Refluxing solutions of pure **1a**–**e** in benzene lead to the formation of **2a**–**e** in better yields and with shorter reaction times of 15–30 min (Reaction 2 in Scheme 1). In contrast, $[Fe(PBu^n_3)_2(CO)_2(\eta^2\text{-}CS_2)]$ can be recovered unchanged in near quantitative yields from this reaction.

Stability of 2 as a function of L

Ligand size appears to play an important role in stabilising **2**. Those which can be isolated have phosphorus(III) ligands L with cone angles[16] which lie between 109° {L = $P(OEt)_3$} and 133° {L = $PPh_2(OEt)$ }. The most stable complexes, which are also those formed in highest yields, have L = $P(OPh)_3$ and $P(OPr^i)_3$ where cone angles[16] are 128° and 130° respectively. With smaller L {PMe_3, $P(OMe)_3$, $P(OCH_2)_3CMe$ and PBu^n_3}, only $[Fe(L)(CO)_4]$ or $[Fe(L)_2(CO)_2(\eta^2\text{-}CS_2)]$ could be identified in the reaction mixtures. Larger L {PPh_3, $P(C_6H_4Me\text{-}4)_3$, $P(C_6H_4OMe\text{-}4)_3$ and $P(OC_6H_4Cl\text{-}4)_3$} give highly coloured products which are not **2**.

The structures of $[Fe_2\{P(OPh)_3\}_4(CO)_2(C_2S_4)]$ (2a) and $[Fe_2\{P(OPr^i)_3\}_4(CO)_2(C_2S_4)]$ (2c)

X-Ray diffraction was used to determine the structures of **2a** and **2c**. The structures are illustrated in Fig. 1 and 2 together with the atom labelling. Selected bond lengths and angles are listed in Table 2.

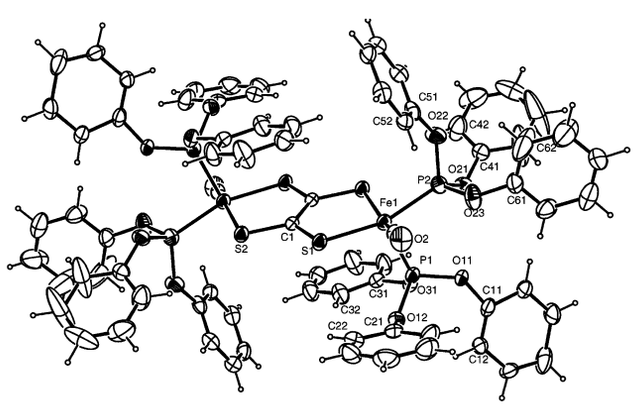

Fig. 1 The molecular structure and atom labelling of $[Fe_2\{P(OPh)_3\}_4(CO)_2(C_2S_4)]$, **2a**.

Both molecules are centrosymmetric with a C_2S_4 ligand acting as a 1,2-dithiolene to two five-coordinate Fe atoms whose ligand sets are completed by one CO and two phosphite ligands. Despite their overall similarities, there are subtle differences between the two structures. In **2c** coordination about Fe is a somewhat distorted trigonal bipyramid with S(1), P(1) and P(2) lying in the equatorial plane (sum of angles = 360.00°), a small P(1)–Fe–P(2) angle of 93.56(7)°, and the tetrathiolene spanning axial and equatorial sites, and $C(2)\text{–}Fe\text{–}S(2a)_{axial}$ = 174.7(2)°. The Fe–S distances are different, $Fe(1)\text{–}S(2a)_{axial}$ > $Fe(1)\text{–}S(1)_{eq}$ {2.2132(17) *vs.* 2.1799(17) Å} as are the two Fe–P bond lengths, Fe(1)–P(2) > Fe(1)–P(1) {2.1452(17) *vs.* 2.1275(18) Å}. A similar coordination polyhedron about Fe is

Table 2 Selected bond lengths (Å) and angles (°) for $[Fe_2\{P(OPh)_3\}_4(CO)_2(C_2S_4)]$, **2a**, and $[Fe_2\{P(OPr^i)_3\}_4(CO)_2(C_2S_4)]$, **2c**.

	2a	**2c**
Fe(1)–C(2)	1.771(5)	1.747(6)
Fe(1)–P(1)	2.1298(15)	2.1275(18)
Fe(1)–P(2)	2.1714(15)	2.1452(17)
Fe(1)–S(1)	2.2201(14)	2.1799(17)
Fe(1)–S(2a)	2.1967(15)	2.2132(17)
C(1)–S(1)	1.732(4)	1.736(5)
C(1)–S(2)	1.736(4)	1.724(5)
C(1)–C(1a)	1.384(7)	1.365(10)
C(2)–O(2)	1.152(5)	1.154(7)
C(2)–Fe(1)–P(1)	95.86(13)	90.9(2)
C(2)–Fe(1)–P(2)	88.77(13)	93.5(2)
C(2)–Fe(1)–S(1)	87.60(13)	86.3(2)
C(2)–Fe(1)–S(2a)	158.26(13)	174.7(2)
P(1)–Fe(1)–P(2)	95.08(6)	93.56(7)
P(1)–Fe(1)–S(1)	103.82(6)	130.88(7)
P(1)–Fe(1)–S(2a)	105.86(5)	90.37(6)
P(2)–Fe(1)–S(1)	161.02(5)	135.56(7)
P(2)–Fe(1)–S(2a)	88.43(5)	91.56(6)
S(1)–Fe(1)–S(2a)	88.07(5)	88.97(6)
Fe(1)–S(1)–C(1)	106.80(12)	106.30(19)
Fe(1)–S(2a)–C(1a)	106.66(12)	105.28(19)
C(1a)–C(1)–S(1)	118.4(4))	119.1(5)
C(1)–C(1a)–S(2a)	119.8(4	120.3(5)
S(1)–C(1)–S(2)	121.8(2)	120.6(3)

Symmetry transformations used to generate equivalent atoms: $-x, -y, -z$.

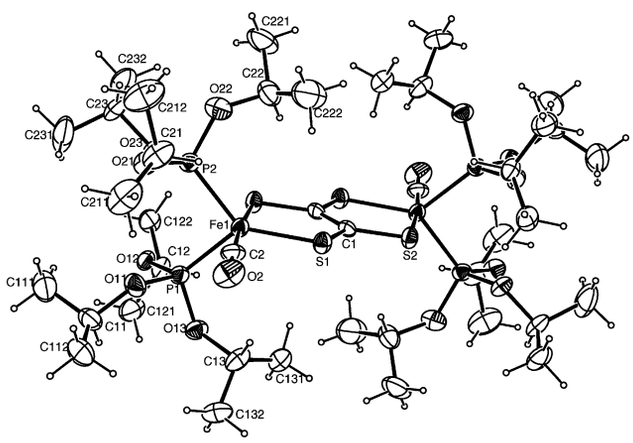

Fig. 2 The molecular structure and atom labelling of $[Fe_2\{P(OPr^i)_3\}_4(CO)_2(C_2S_4)]$, **2c**.

found in the mononuclear dithiolene derivative $[Fe\{P(OMe)_3\}_2(CO)\{S_2C(COMe)C(C_6H_4NO_2)\}]$ (equatorial angle sum = 359.8° and *trans* angle = 173.6°) where the Fe–S distances are somewhat shorter than those in **2c**, but again $Fe–S_{axial} > Fe–S_{eq}$ {2.196(1) *vs.* 2.155(1) Å}.[17]

In **2a**, on the other hand, the coordination about Fe is close to a square-based pyramid. P(1) occupies the axial site, but is bent back from the tetrathiolene ligand {both S–Fe–P(2) = *ca.* 105°, but P(1)–Fe(1)–P(2) = 95.08(6)° and P(1)–Fe(1)–C(2) = 95.86(13)°} and the basal *trans* angles are similar at *ca.* 160°. The two Fe–S distances are somewhat different with Fe(1)–S(1) > Fe(1)–S(2a) {2.2201(14) *vs.* 2.1967(15) Å} whilst $Fe(1)–P(2)_{eq} > Fe(1)–P(1)_{axial}$ {2.1714(15) *vs.* 2.1298(15) Å}. A similar coordination is found in the dithiolene complex $[Fe(PPh_3)(CO)_2\{S_2C_2(SMe)_2\}]$ with an axial CO ligand,[7] and in the centrosymmetric tetrathiolene derivative $[Rh_2\{(Ph_2PCH_2)_3CMe\}_2(C_2S_4)]^{2+}$ where $M–P_{eq}$ is also greater than $M–P_{axial}$.[5]

The $S_2C_2S_2$ ligands in **2a** and **2c** are planar and the iron atoms lie close to that plane. A similar arrangement is found in $[Ni_2(\eta^5\text{-}C_5Me_5)_2(C_2S_4)]$[3] but not in $[Rh_2\{(Ph_2PCH_2)_3CMe\}_2(C_2S_4)]^{2+}$ where the metal atoms are *ca.* 0.3 Å out of that plane.[5]

The C–C distances are similar, 1.384(7) Å in **2a** and 1.365(10) Å in **2c**. They are comparable to those for other tetrathiolenes *e.g.* 1.37(3) Å in $[Rh_2\{(Ph_2PCH_2)_3CMe\}_2(C_2S_4)]^{2+}$,[5] 1.342(8) Å in $[Rh_2(\eta^5\text{-}C_5Me_5)_2(C_2S_4)]$,[6] and 1.360(11) Å in $[Ni_2(\eta^5\text{-}C_5Me_5)_2(C_2S_4)]$,[5] and mononuclear dithiolenes {1.355(5) Å in $[Fe(PPh_3)(CO)_2\{S_2C_2(SMe)_2\}]$[7] and 1.390(15) Å in $[Fe\{P(OMe)_3\}_2(CO)\{S_2C(COMe)C(C_6H_4NO_2)\}]$[16]}. They are much shorter than the 1.447(13) Å found in the tetrathiooxalate ligand of $[Rh_2(\eta^5\text{-}C_5Me_5)_2Cl_2(C_2S_4)]$,[7] but longer than the 1.33(1) Å in the ethenetetrathiolate ligand of $[Fe_2(CO)_6\}_2(\mu\text{-}C_2S_4)]$.[2] They lie between the values for C=C and C–C between sp^2 C atoms (1.32 and 1.46 Å respectively),[18] as do the C–S bond lengths (1.67 Å and 1.80 Å[18]). These bond lengths are consistent with a delocalised quasi-aromatic bonding in the FeS_2C_2 ring so that if the dithiolenes $L_3FeS_2C_2R_2$ are counterparts of benzene, the tetrathiolene complexes, **2**, may be considered as analogues of naphthalene with ten π electrons (Fig. 3).

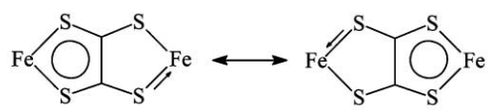

Fig. 3 Some of the possible mesomers of **2**.

Spectroscopic characterisation of 2

The spectra of all **2** are consistent with centrosymmetric molecular structures similar to those of **2a** and **2c** in both solid state and solution. In the IR spectra there were no absorption bands with frequencies > 400 cm^{-1} (KBr discs) which could be assigned with confidence to vibrations of the $FeS_2C_2S_2Fe$ moiety whilst the single *ν*(CO) band shows the anticipated frequency variation on changing the ancillary phosphorus ligands.

The ^{31}P NMR spectra of **2** show a single resonance, which indicates that all four phosphorus ligands are equivalent on the NMR time-scale. In **2a** at least there are two types of P ligands, so clearly these compounds are fluxional, possibly by the Berry pseudo-rotation process or a turnstile rotation of the $Fe(L)_2CO$ moiety. A similar situation has been observed for $[\eta^3\text{-}\{MeC(CH_2PPh_2)_3\}Rh(S_2C_2S_2)Rh\{(Ph_2PCH_2)_3CMe\}\text{-}\eta^3]^{2+}$.[5]

^{13}C NMR spectra could only be obtained for **2a** and **2c**. For both, the CO ligands give rise to a single resonance which is a triplet due to coupling to the two ^{31}P nuclei coordinated to the same Fe atom, with a J_{PC} of 31.1 Hz {L = $P(OPh)_3$} and 36.0 Hz {L = $P(OPr^i)_3$}. The C atoms of the tetrathiolene ligands give rise to singlet resonances at *δ* 193.8 for **2a** and *δ* 183.5 for **2c** which are slightly broadened with any coupling to ^{31}P unresolved. These chemical shifts are similar to the *δ* 169.4 found for the tetrathiolene complex $[Rh_2(\eta\text{-}C_5H_5)_2(C_2S_4)]$[6] and different from the *δ* 234.7 for the tetrathiooxalato derivative $[Rh_2(\eta\text{-}C_5H_5)_2Cl_2(C_2S_4)]$.[6]

Tetrathiolene complexes are highly coloured {*e.g.* $[\eta^3\text{-}\{MeC(CH_2PPh_2)_3\}Rh(S_2C_2S_2)Rh\{(Ph_2PCH_2)_3CMe\}\text{-}\eta^3]^{2+}$ salts are green,[5] and $[(\eta^5\text{-}C_5Me_5)Rh(S_2C_2S_2)Rh(\eta^5\text{-}C_5Me_5)]$ is blue (λ_{max} = 688 nm)[6]}. **2** are blue-purple and their electronic spectra all show a low-energy absorption band (λ_{max} = 640–690 nm) of high intensity (ε = 13,000–18,000 $dm^3\ mol^{-1}\ cm^{-1}$) which is attributed to a MLCT transition within their $Fe(S_2C_2S_2)Fe$ cores. Similar absorption bands are observed in the UV-Vis spectra of mononuclear $[Fe(L)_3(S_2C_2R_2)]$ dithiolene derivatives {*e.g.* $[Fe(Ph_2PCH_2CH_2PPh_2)(CO)\{S_2C_2(CF_3)_2\}]$ is purple (λ_{max} = 568 nm, ε = 2,100 $dm^3\ mol^{-1}\ cm^{-1}$) and $[Fe\{P(OEt)_3\}_2(CO)\{S_2C_2(CF_3)_2\}]$ dark red (λ_{max} = 518 nm, ε = 1,880 $dm^3\ mol^{-1}\ cm^{-1}$)}, but are of higher energy and are less intense. This is attributed to the more extensive delocalisation in the binuclear compounds. A similar situation is observed in going from benzene to naphthalene.[19]

In $[Fe(L)_3(S_2C_2R_2)]$ complexes, the wavelength of the CT bands increases for L = CO < $P(OEt)_3$ < CNR < PPh_3.[8] A

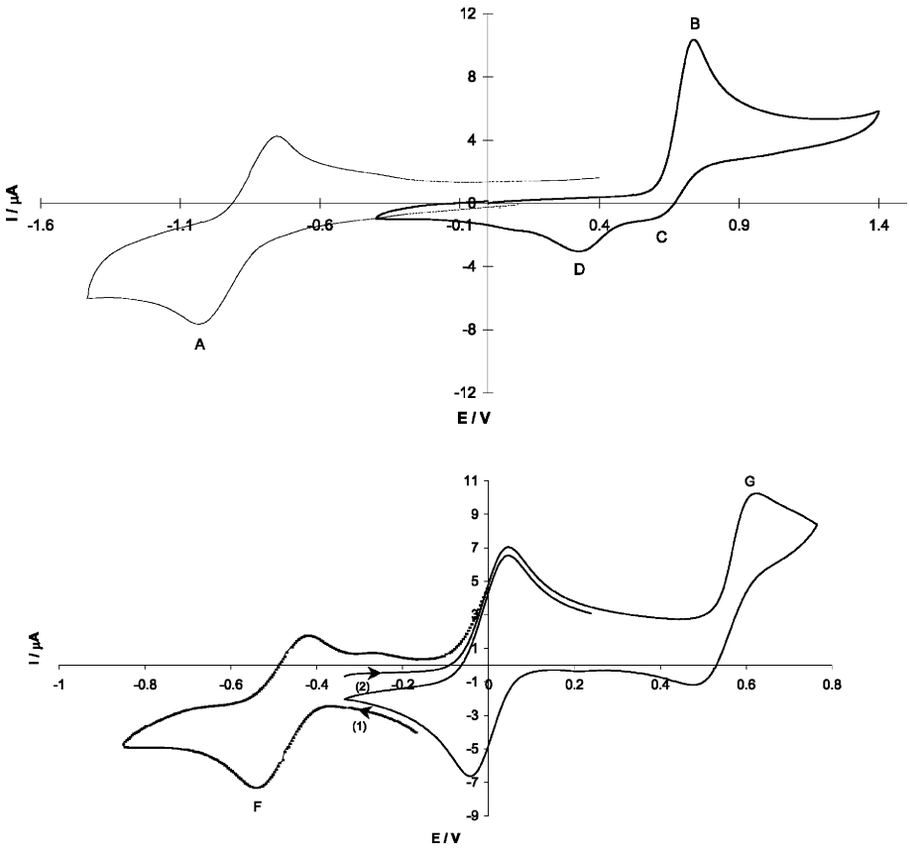

Fig. 4 Cyclic voltammogram of **2a** (CH_2Cl_2, Pt, 800 mV s^{-1}, 293 K, 0.1 M Et_4NClO_4) under Ar (above) and CO (below) (decamethylferrocene couple at 0.0 V).

similarly straightforward relationship does not exist for **2** as these divide themselves into two groups. The first has λ_{max} = 640–650 nm where L = $P(OEt)_3$ (640), and $P(OPr^i)_3$ (642), whilst the second has λ_{max} = 667–690 nm where L = $P(OEt)_2Ph$ (671), $P(OPh)_3$ (677) and $P(OEt)Ph_2$ (686). It is possible that this subdivision reflects differing coordination geometries about iron, and that **2d** and **2e** have square-based pyramidal geometry like **2a** whilst **2b** has trigonal bipyramidal coordination like **2c**.

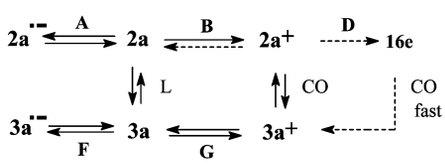

Scheme 2

Reaction of $[Fe_2\{P(OPh)_3\}_4(CO)_2(C_2S_4)]$ (2a) with CO

The phosphite ligands of **2a** are labile. When CO is passed through its solution for 5 min there is a slight colour change and the ν(CO) band of **2a** is replaced by two bands at higher frequencies due to a new species **3a**. This reverts to **2a** on removal of the CO by a stream of nitrogen and only **2a** can be isolated from the mixture on removal of the solvent at reduced pressure. If the reverse reaction is prevented by removal of $P(OPh)_3$ from the equilibrium by addition of $[Ph_3C]BF_4$, **3a** may be isolated as a blue solid, but it is unstable and decomposes even in the solid state to **2a** and other products, so it was characterised by spectroscopic methods alone. The UV-Vis spectrum of **3a**, and the ease with which **2a** and **3a** interconvert suggest that **3a** retains the $Fe(S_2C_2S_2)Fe$ tetrathiolene nucleus intact. The presence of two ν(CO) IR bands at somewhat higher frequencies than those of **2a** suggest that **3a** is $[Fe_2\{P(OPh_3)\}_n(CO)_{6-n}(C_2S_4)]$ with $n < 4$. On the basis of the spectroscopic data taken as a whole, the most plausible formulation for **3a** has $n = 3$.

Redox chemistry of 2a

Square-wave and cyclic voltammetry of **2a** in CH_2Cl_2 over the potential range −1.6 to 1.4 V shows one cathodic process (**A**), E° = −0.87 V against decamethylferrocene, and one anodic process (**B**) E_{ap} = 0.71 V (Fig. 4, Scheme 2). Each has electrochemical parameters which are compatible with one-electron transfers. In this respect the redox chemistry of **2a** is relatively simple compared to that observed for the isoelectronic $[\eta^3\text{-}\{MeC(CH_2PPh_2)_3\}Rh(\mu\text{-}C_2S_4)Rh\{(Ph_2PCH_2)_3CMe\}\text{-}\eta^3]^{2+}$,[5] and different from that of another isoelectronic molecule, $[(\eta^5\text{-}C_5Me_5)Rh(\mu\text{-}C_2S_4)Rh(\eta^5\text{-}C_5Me_5)]$, where the equivalent **B/A** current ratio is 2 : 1.[6,20]

Process **A** is chemically reversible with i_{pa}/i_{pc} = 1.0 at 200 mV s^{-1} and $i_p/v^{-1/2}$ is constant over the scan range 50 mV s^{-1} to 1 V s^{-1} irrespective of the initial scan direction. At slower rates i_{pa}/i_{pc} may be as low as 0.8 but this is due to the rapid fouling of the Pt and carbon electrodes that is pervasive at slow scans. **A** is assigned to the reversible formation of the radical anion $[\mathbf{2a}]^{\bullet-}$. The potential of $E^\circ[\mathbf{2a}]^{0/-1}$ = −0.87 V is the same as that for $[\{Co(\eta^5\text{-}C_5H_5)\}_2Fe(L)_2(\mu_3\text{-}S)(\mu_3\text{-}C_2S_3)]$,[21] and similar to those for $[\eta^3\text{-}\{MeC(CH_2PPh_2)_3\}Rh(\mu\text{-}C_2S_4)Rh\{(Ph_2PCH_2)_3CMe\}\text{-}\eta^3]^{2+}$ (−0.90 V)[5] and $(\eta^5\text{-}C_5Me_5)Rh(\mu\text{-}C_2S_4)Rh(\eta^5\text{-}C_5Me_5)$ (−0.82 V).[6,20]

In order to gain an insight into the nature of the singly occupied molecular orbital (SOMO) of $[\mathbf{2a}]^{\bullet-}$, isotropic ESR spectra were recorded at 280 and 250 K and a frozen solution spectrum, shown in Fig. 5, at 120 K. The isotropic spectrum is a 1 : 2 : 1 triplet with $\langle g \rangle$ = 2.0388 and $\langle A \rangle$ = 85.2 × 10^{-4} cm^{-1} at both temperatures. Large couplings such as this are unusual[22] (20–30 × 10^{-4} are more common[23]) and generally signify that the phosphorus ligand(s) is (are) located essentially on a lobe of the SOMO,[22] whilst the triplet nature of the ESR signal suggests that the SOMO is confined to one Fe atom. As the iron

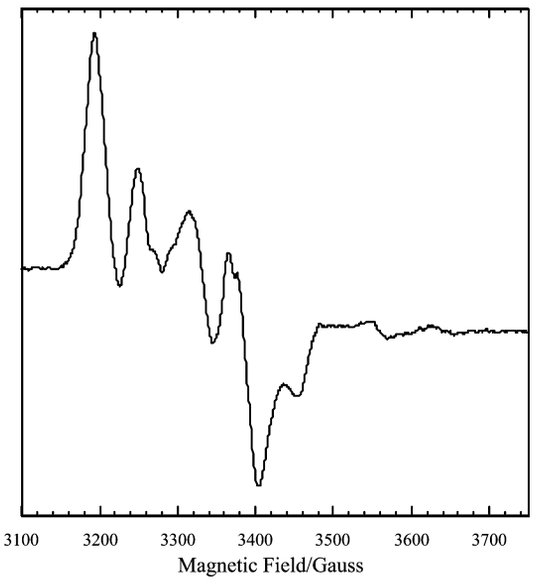

Fig. 5 Anisotropic ESR spectrum of $\mathbf{2a}^{\bullet-}$ in a CH_2Cl_2 glass at 120 K.

has a nominal oxidation state of +1, crystal field arguments predict that the SOMO is primarily Fe $d_{x^2-y^2}$ in character. The frozen solution spectrum is poorly resolved, but can be interpreted in terms of nearly axial *g*-matrix, $g = 2.005, 2.048, 2.58$ (all ± 0.001) and rhombic *A*-matrices, $A_1 = 115, 62, 115$, $A_2 = 61, 121, 51$ (all ± 2×10^{-4} cm^{-1}). An axial *g*-matrix would be expected if the SOMO were purely $d_{x^2-y^2}$, but a small admixture of d_{z^2} would lead to the observed departure from axial symmetry. The phosphine ligands are clearly non-equivalent in the frozen solution spectrum. This is consistent with the square pyramidal coordination about the Fe atom in **2a** in which phosphorus atoms occupy axial, P(2), and basal sites, P(1) (Fig. 1). The apparent equivalence in the isotropic spectra is probably a consequence of the rather broad lines (peak-to-peak linewidths of *ca.* 20 G).

When **2a** is reduced to $\mathbf{2a}^{\bullet-}$ in an OTTLE cell, UV/Vis profiles showed reversible changes with good isosbestic points (Fig. 6). The significant absorption band of **2a** (677 nm) is red-shifted to 765 nm in $[\mathbf{2a}]^{\bullet-}$. This is accompanied by the appearance of a remarkably low energy band at 2556 nm (3912 cm^{-1}) with an intensity ε = *ca.* 3600 dm^3 mol^{-1} cm^{-1}. Its large bandwidth ($\Delta\nu_{1/2}$ = 400 cm^{-1}) and weakly positive solvatochroism are compatible with a charge-transfer transition from the more polar SOMO on the reduced metal centre to a delocalised orbital based on the (μ-C_2S_4) ligand.

The anodic process **B** at 0.71 V due to the formation of $\mathbf{2a}^{+}$ is chemically irreversible between 223 and 293 K, and in the scan range 0.05 V s^{-1} to 1 V s^{-1}. A small companion cathodic component **C** is discernible at 0.63 V. The current ratio *i*(**D**)/*i*(**B**) for the major feature on the cathodic scan **D** at 0.33 V is 0.16 at

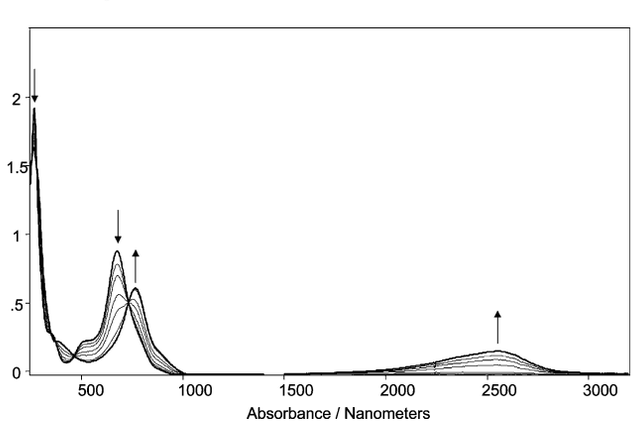

Fig. 6 UV/Vis OTTLE spectrum (Pt electrode, 293 K, CH_2Cl_2, −0.9 V) of **2a** and $\mathbf{2a}^{\bullet-}$ (400–3000 nm).

100 mV s^{-1}, with only a small increase in this ratio at 1 V s^{-1}; *i*(**D**)/*i*(**B**) changes little with temperature although the difference in potential between **B** and **D** increases as the temperature is lowered. This behaviour is symptomatic of a molecule undergoing a slow structural change concomitant upon oxidation to the cation.[24] Two such rearrangements have been proposed for isoelectronic molecules; an oxidative dimerisation[20] for (η^5-C_5Me_5)Rh(C_2S_4)Rh(η^5-C_5Me_5) and a conformational change plus rearrangement[5] from an ethenetetrathiolate to a tetrathiolate group for [{η^3-MeC(CH_2PPh_2)$_3$}Rh(μ-C_2S_4)Rh{η^3-(PPh_2CH_2)$_3$CMe}]$^{2+}$. Oxidative dimerisation requires an *i*(**A**) : *i*(**B**) ratio of 1 : 2 and an ethenetetrathiolate/tetrathiolate interconversion, which is not compatible with the spectroelectrochemical data. Upon oxidation of **2a** in a UV/Vis OTTLE cell the 675 nm band is replaced by a broad transition centred at 663 nm. This suggests that the structural change **B** ⟶ **D** does not significantly perturb the energy levels of the L_2(CO)FeS_2 unit. An IR OTTLE experiment showed that the new species formed during the oxidation of **2a** at 0.8 V (in the timeframe of the OTTLE experiment this is **D**) has *ν*(CO) bands at 2077 (w), 2020 (s) cm^{-1} (Fig. 7). This profile is typical of an oxidised Fe$(CO)_3$ group or a Fe(L)$(CO)_2$ moiety in which the C–Fe–C angle is *ca.* 120°.[25] Slow phosphine dissociation and/or CO transfer is not uncommon from oxidised 18e metal carbonyl species[26] so **D** could be assigned to [$Fe_2(L)_n$-$(CO)_{6-n}(C_2S_4)$]$^+$ species where $n < 4$ although E^0(**D**) should not be < E^0(**B**).

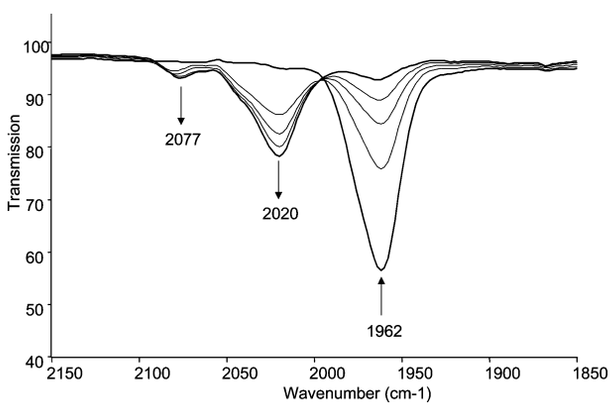

Fig. 7 IR OTTLE spectrum (Pt electrode, 293 K, CH_2Cl_2, +0.8 V) of **2a**.

To probe the relationship between the redox chemistry and the **2a**/CO chemistry described above, the spectroelectrochemistry was repeated under CO. First, the one-electron reduction process **A** shifts to −0.48 V (**F**) but remains chemically reversible (again, rapid electrode fouling occurs); this is followed by a complex series of irreversible electron transfers > −0.9 V. Previous work[27] has shown that a 390 mV shift is indicative of the replacement of *one* phosphite ligand by CO due to a reduction of the electron density around the metal centre. Moreover, the electrode thermodynamics allow for ETC (ECE) substitution as well; with this mechanism the substitution of more than one CO per Fe is unlikely.[26] Therefore, the electron transfer at **F** is assigned to the formation of the radical anion $\mathbf{3a}^{\bullet-}$ (see Scheme 2). The second effect occurs in the anodic region. Here, **B** in **2a** undergoes a *cathodic* shift to 0.55 V (**G**) and the one-electron transfer becomes *chemically reversible* (Fig. 4). Moreover, E_{pc}(**G**) ≅ E_{pc}(**D**). The species giving rise to this reversible couple **G** is logically that discussed above for the reduction, **3a**, and this is confirmed by an IR OTTLE *ν*(CO) spectrum. However, as noted above for **D**, this assignment runs counter to the reduced electron density on the Fe when a phosphorus(III) ligand is replaced by CO. This suggests that there is a structural modification as well as CO substitution upon oxidation of **3a** which changes the character of the HOMO. An ethenetetrathiolate/tetrathiolate change is unlikely

to increase the electron density on the Fe to account for the **B** to **G** shift in potential. We suggest that in **3a** the electron density on the iron atoms is increased by intermolecular S ⟶ Fe similar to those observed for $[Fe(CO)_3\{S_2C_2(CF_3)_2\}]_2$.[28] When CO is replaced by phosphorus ligands these intermolecular interactions are inhibited.

Chemical oxidation of 2a with halogen

In the light of the successful halogenation of $[(\eta^5\text{-}C_5Me_5)Rh(\mu\text{-}C_2S_4)Rh(\eta^5\text{-}C_5Me_5)]$ to $[(\eta^5\text{-}C_5Me_5)(Cl)Rh(\mu\text{-}C_2S_4)Rh(Cl)(\eta^5\text{-}C_5Me_5)]$,[6] and the electrochemical studies discussed above, we investigated the reactions of **2a** with halogens, X_2 = (i) Cl_2 (as $PhICl_2$), (ii) Br_2 (as $C_5H_5NHBr_3$), and (iii) I_2. These give green solutions from which could be isolated green solids **4a** that would not redissolve in any solvent. **4a** and their soluble precursors react with methyllithium to regenerate **2a** in reactions which appeared to be *ca*. quantitative by IR spectroscopy and from which could be isolated pure **2a** in *ca*. 70–80% yields. Although the solid **4a** could not be further purified, they analyse reasonably well for $[Fe_2\{P(OPh)_3\}_4(CO)_2(C_2S_4)X_2]$, where X = Cl, Br and I. Similar compounds are formed on the reaction of **2c** with halogens but are much less stable than **4a**.

The comparable reaction of the tetrathiolene complex $[(\eta\text{-}C_5Me_5)Rh(S_2C_2S_2)Rh(\eta\text{-}C_5Me_5)]$ with chlorine gives $[(\eta\text{-}C_5Me_5)(Cl)Rh(S_2C_2S_2)Rh(Cl)(\eta\text{-}C_5Me_5)]$.[6] There is an increase in the coordination number of the Rh atoms, and the nature of the bridging C_2S_4 changes from a tetrathiolene 8-electron donor to a tetrathiooxalato 6-electron donor. By analogy, we suggest that **4a** is also a tetrathiooxalate complex with six-coordinate iron atoms. The presence of a single *ν*(CO) band in the IR spectra of **4a** suggests that the centrosymmetric structure is retained whilst its relatively high frequency is consistent with a higher effective oxidation state of Fe. Unfortunately, the NMR spectra of **4a** could not be obtained due to solubility problems. The conversions of $[(\eta\text{-}C_5Me_5)Rh(S_2C_2S_2)Rh(\eta\text{-}C_5Me_5)]$ to $[(\eta\text{-}C_5Me_5)(Cl)Rh(S_2C_2S_2)Rh(Cl)(\eta\text{-}C_5Me_5)]$ and of **2a** to **4a** both result in colour changes from blue to green. The UV-Vis spectra of **4a** show that this is due to a high intensity absorption band at *ca*. 700–750 nm depending on the halogen. The high intensity and low energies of these bands suggest that the bonding in the $Fe(S_2C_2S_2)Fe$ moiety of **4a** and **5a** is also delocalised.

Acknowledgements

We thank Professor W. T. Robinson (University of Canterbury) for the X-ray data collection and Dr Joy Morgan for assistance.

References

1 P. Conway, S. M. Grant and A. R. Manning, *J. Chem. Soc., Dalton Trans.*, 1979, 1920.
2 P. V. Broadhurst, B. F. G. Johnson, J. Lewis and P. R. Raithby, *J. Chem. Soc., Chem. Commun.*, 1982, 140.
3 H. A. Harris, A. D. Rae and L. F. Dahl, *J. Am. Chem. Soc.*, 1987, **109**, 4739.
4 J. J. Maj, A. D. Rae and L. F. Dahl, *J. Am. Chem. Soc.*, 1982, **104**, 4278.
5 C. Bianchini, C. Mealli, A. Meli, M. Sabat and P. Zanello, *J. Am. Chem. Soc.*, 1987, **109**, 185.
6 G. A. Holloway and T. B. Rauchfuss, *Inorg. Chem.*, 1999, **38**, 3018.
7 D. Touchard, J.-L. Fillaut, D. V. Khasnis, P. H. Dixneuf, C. Mealli, D. Masi and L. Toupet, *Organometallics*, 1988, **7**, 67.
8 J. A. McCleverty, *Prog. Inorg. Chem.*, 198, **10**, 49; J. Miller and A. L. Balch, *Inorg. Chem.*, 1971, **10**, 1410.
9 R. B. King, *Organomet. Synth.*, 1965, **1**, 93.
10 M. C. Baird, G. Hartwell and G. Wilkinson, *J. Chem. Soc. A*, 1967, 2037.
11 M. R. Waterland and K. C. Gordon, *J. Raman Spectrosc.*, 2000, **31**, 243–253.
12 SMART and SAINT: Area detector control and integration software, Bruker AXS, Madison, WI, 1994.
13 SADABS (*absorption correction for area detector data)*, Bruker AXS, Madison, WI, 1997.
14 G. M. Sheldrick, SHELXS-97, A program for the solution of crystal structures from diffraction data, University of Göttingen, Germany, 1990; SHELXL-97, A program for the refinement of crystal structures, University of Göttingen, Germany, 1997.
15 K. A. Hunter and J. Simpson, TITAN2000, A molecular graphics program to aid structure solution and refinement with the SHELX suite of programs, University of Otago, Dunedin, New Zealand, 1999.
16 C. A. Tolman, *Chem. Rev.*, 1977, **77**, 313.
17 A. J. Carty, P. H. Dixneuf, A. Gorgues, F. Hartstock, H. Le Bozec and N. J. Taylor, *Inorg. Chem.*, 1981, **20**, 3929.
18 F. H. Allen, O. Kennard, D. G. Watson, L. Brammer, A. G. Orpen and R. Taylor, *J. Chem. Soc., Perkin Trans. 2*, 1987, S1–S19.
19 E. Clar, *Polycyclic Hydrocarbons, Volume 1*, Academic Press, London and New York, 1964.
20 G. A. Holloway, K. K. Klausmeyer, S. R. Wilson and T. B. Rauchfuss, *Organometallics*, 2000, **19**, 5370.
21 A. R. Manning, A. J. Palmer, C. J. McAdam, B. H. Robinson and J. Simpson, unpublished work.
22 J. A. DeGray, Q. Meng and P. H. Rieger, *J. Chem. Soc., Faraday Trans. 1*, 1987, **83**, 3565.
23 D. A. Cummings, J. McMaster, A. L. Rieger and P. H. Rieger, *Organometallics*, 1997, **16**, 4362.
24 B. Tulyathan and W. E. Geiger, *J. Am. Chem. Soc.*, 1985, **107**, 5970.
25 W. Beck, A. Melnikoff and R. Stahl, *Chem. Ber.*, 1966, **99**, 3721.
26 B. H. Robinson and J. Simpson, in *Paramagnetic Organometallic Species in Activation/Selectivity Catalysis*, ed. M. Chanon, Kluwer, Dordrecht, 1989, p. 357.
27 N. W. Duffy, C. J. McAdam, B. H. Robinson and J. Simpson, *J. Organomet. Chem.*, 1998, **565**, 19.
28 C. J. Jones, J. A. McCleverty and D. G. Orchard, *J. Chem. Soc., Dalton Trans.*, 1972, 1109.